

## HIGH-ORDER PHOTON-NUMBER CORRELATIONS: A RESOURCE FOR CHARACTERIZATION AND APPLICATIONS OF QUANTUM STATES

ALESSIA ALLEVI

*Dipartimento di Scienza e Alta Tecnologia,  
Università degli Studi dell'Insubria and C.N.I.S.M.,  
U.d.R. Como, Via Valleggio 11, Como I-22100, Italy  
[alessia.allevi@uninsubria.it](mailto:alessia.allevi@uninsubria.it)*

STEFANO OLIVARES

*Dipartimento di Fisica,  
Università degli Studi di Milano and C.N.I.S.M.,  
U.d.R. Milano Statale, Via Celoria 16, Milano I-20133, Italy  
[stefano.olivares@fisica.unimi.it](mailto:stefano.olivares@fisica.unimi.it)*

MARIA BONDANI

*Istituto di Fotonica e Nanotecnologie,  
Consiglio Nazionale delle Ricerche and C.N.I.S.M.,  
U.d.R. Como, Via Valleggio 11, Como I-22100, Italy  
[maria.bondani@uninsubria.it](mailto:maria.bondani@uninsubria.it)*

Received 8 October 2012

Accepted 2 November 2012

Published 11 January 2013

We measure high-order correlation functions of detected-photon numbers in the mesoscopic regime by means of hybrid photodetectors. The analytical expressions for correlations are evaluated in terms of quantities that can be experimentally accessed by a selfconsistent analysis of the detectors' outputs. We demonstrate that high-order correlations can be used to characterize the nature of the optical states, for instance by better discriminating between classical and quantum behavior even in critical situations, such as multimode twin-beam state. The results are in very good agreement with the theory, both for classical states and quantum states.

*Keywords:* Quantum optics; photon statistics; quantum state engineering and measurements; light detectors.

PACS Number(s): 42.50.Ar, 42.50.Dv, 85.60.Gz

## 1. Introduction

Photon-number correlation functions, introduced by Glauber in 1963,<sup>1</sup> have become a useful tool for basic investigation of optical coherence<sup>2</sup> and nonclassicality<sup>3</sup> and for applications to the enhancement of ghost-imaging protocols.<sup>4–7</sup>

Glauber’s correlation functions are defined in terms of normal ordered operators and their expression are not accessible by realistic (non-perfect detection efficiency) direct detection schemes. To have a direct link to experimental results, we recently<sup>8</sup> introduced the analytical expression of correlation functions in terms of detected photons for several classical and quantum states and used them to fully characterize a multimode twin-beam state in comparison with its classical counterpart, that is a multimode thermal state. To this aim we also introduced a nonclassicality criterion based on a simple linear combination of high-order correlation functions that enhances the discrimination capability of quantum states in critical situations, such as for highly multimode states detected with low quantum efficiency.<sup>8</sup> The experimental implementation takes advantage of a direct detection scheme based on hybrid photodetectors,<sup>9,10</sup> which yields the determination of shot-by-shot numbers of detected photons and all the relevant physical parameters (quantum efficiency, number of modes and average energy) from the same experimental data.<sup>11,12</sup>

In this paper we present the characterization in terms of high-order correlations of a classical state obtained by coherently displacing a phase-averaged coherent state (D-PHAV hereafter) that has recently come to interest as it is a non-Gaussian state useful for quantum information applications<sup>13–16</sup>. We then compare D-PHAV states to both the multimode twin beam and the multimode pseudothermal states, showing the usefulness of high-order correlations in the discrimination among similar states.

## 2. Theory

The correlation functions  $g_{\hat{n}}^{jk}$  defined in terms of the normally-ordered creation and annihilation operators,<sup>17</sup>

$$g_{\hat{n}}^{jk} = \frac{\langle : \hat{n}_1^j \hat{n}_2^k : \rangle}{\langle : \hat{n}_1 : \rangle^j \langle : \hat{n}_2 : \rangle^k} = \frac{\langle \hat{a}_1^\dagger{}^j \hat{a}_1^j \hat{a}_2^\dagger{}^k \hat{a}_2^k \rangle}{\langle \hat{a}_1^\dagger \hat{a}_1 \rangle^j \langle \hat{a}_2^\dagger \hat{a}_2 \rangle^k}, \quad (1)$$

where  $\hat{a}_i$  is the field operator of the mode  $i$ th and  $\hat{n}_i = \hat{a}_i^\dagger \hat{a}_i$ , have a well-recognized meaning in connection with coherence properties of light and  $n$ -photon absorption process,<sup>18</sup> but unfortunately cannot be accessed by realistic direct detection schemes. To establish a link between correlation functions and directly detected quantities, we define the following “detected-photons” correlation functions<sup>8</sup>

$$g_{\hat{m}}^{jk} = \frac{\langle \hat{m}_1^j \hat{m}_2^k \rangle}{\langle \hat{m}_1 \rangle^j \langle \hat{m}_2 \rangle^k}, \quad (2)$$

in which  $\hat{m}_i$  is the operator describing the actual number of detected photons in a shot-by-shot measurement in the  $i$ th arm of the bipartite state. As expected, the

functions  $g_{\hat{m}}^{jk}$  can be linked to the  $g_n^{jk}$  of Eq. (1), provided that a suitable description of the actual operation performed by the detector is given.

According to the results presented in Ref. 8, the correlation functions of Eq. (2) evaluated for a multimode twin beam take the form:

$$g_{\hat{m}}^{11} = G^{(1)}(\mu) + \frac{\eta}{\langle \hat{m} \rangle}, \quad (3a)$$

$$g_{\hat{m}}^{21} = g_{\hat{m}}^{12} = G^{(2)}(\mu) + G^{(1)}(\mu) \frac{1 + 2\eta}{\langle \hat{m} \rangle} + \frac{\eta}{\langle \hat{m} \rangle^2}, \quad (3b)$$

$$g_{\hat{m}}^{22} = G^{(3)}(\mu) + 2G^{(2)}(\mu) \frac{1 + 2\eta}{\langle \hat{m} \rangle} + G^{(1)}(\mu) \frac{1 + 4\eta + 2\eta^2}{\langle \hat{m} \rangle^2} + \frac{\eta}{\langle \hat{m} \rangle^3}, \quad (3c)$$

$$g_{\hat{m}}^{31} = g_{\hat{m}}^{13} = G^{(3)}(\mu) + 3G^{(2)}(\mu) \frac{1 + \eta}{\langle \hat{m} \rangle} + G^{(1)}(\mu) \frac{1 + 6\eta}{\langle \hat{m} \rangle^2} + \frac{\eta}{\langle \hat{m} \rangle^3}, \quad (3d)$$

where  $\langle \hat{m} \rangle$  is the average number of detected photons,  $\mu$  is the number of independent modes,  $\eta$  is the overall detection efficiency and  $G^{(k)}(\mu) = \prod_{k=1}^k (k + \mu) / \mu$ . We remind that Eq. (3) also describes two other classes of states: by choosing  $\eta = 0$  we obtain the correlation functions for a multimode thermal state divided at a beam splitter, while for  $\eta = 0$  and  $\mu \rightarrow \infty$  we get the results for the coherent state divided at a beam splitter.<sup>19</sup> The correlation functions of Eq. (2) for a D-PHAV state divided at a 50% beam splitter take different expressions:

$$g_{\hat{m},D\text{-PHAV}}^{11} = \frac{3}{2}, \quad (4a)$$

$$g_{\hat{m},D\text{-PHAV}}^{21} = g_{\hat{m},D\text{-PHAV}}^{12} = \frac{5}{2} + \frac{3}{2\langle \hat{m} \rangle}, \quad (4b)$$

$$g_{\hat{m},D\text{-PHAV}}^{22} = \frac{35}{8} + \frac{5}{\langle \hat{m} \rangle} + \frac{3}{2\langle \hat{m} \rangle^2}, \quad (4c)$$

$$g_{\hat{m},D\text{-PHAV}}^{31} = g_{\hat{m},D\text{-PHAV}}^{13} = \frac{35}{8} + \frac{15}{2\langle \hat{m} \rangle} + \frac{3}{2\langle \hat{m} \rangle^2}. \quad (4d)$$

We note that  $g_{\hat{m},D\text{-PHAV}}^{11}$  is equal to the expression of  $g_{\hat{m}}^{11}$  obtained for a two-mode thermal field by putting  $\eta = 0$  and  $\mu = 2$  into Eq. (3a) at equal mean photon values. This means that to distinguish between these two cases we need to evaluate higher-order correlations.

To enhance the differences among the various optical states, we now use the functions  $g_{\hat{m}}^{jk}$  to build a new class of correlation functions modeled on the basis of conventional first order correlation function

$$\Gamma_{\hat{m}}^{jk} = (g_{\hat{m}}^{jk} - 1) \frac{\langle \hat{m}_1 \rangle^j \langle \hat{m}_2 \rangle^k}{\sigma_{\hat{m}_1}^j \sigma_{\hat{m}_2}^k}, \quad (5)$$

where  $\sigma_{\hat{m}_i}$  is the square root of the variance of the detected-photon number distribution on the  $i$ th arm.

Finally, we remind here that a new nonclassicality criterion can be built based on high-order correlations<sup>8</sup>:

$$\langle m_1 \rangle \langle m_2 \rangle \frac{g_{\hat{m}}^{22} - [g_{\hat{m}}^{13}]_s}{g_{\hat{m}}^{11}} + \sqrt{\langle m_1 \rangle \langle m_2 \rangle} \frac{[g_{\hat{m}}^{12}]_s}{g_{\hat{m}}^{11}} > 1, \quad (6)$$

where  $[g_{\hat{m}}^{hk}]_s = \frac{1}{2}(g_{\hat{m}}^{hk} + g_{\hat{m}}^{kh})$  is a symmetrized expression. The above inequality must be fulfilled by nonclassical light.

In the following we will compare the results of a multimode twin-beam state with a single-mode thermal state and a D-PHAV and the results of a two-mode thermal state with those of a D-PHAV. Inequality (6) has been tested for multimode twin-beam states in comparison with other nonclassicality criteria, demonstrating the ability of discriminating nonclassical from classical states even in critical situations.<sup>8</sup>

### 3. Experimental Results

The generation of the multimode TWB has already been described in detail elsewhere.<sup>8</sup> Here we remind that the state was generated in non collinear geometry close to frequency degeneracy (signal: 690 nm and idler: 706 nm) by the third harmonics (349 nm wavelength) of a mode-locked Nd:YLF laser regeneratively amplified at 500 Hz (High-Q Laser Production, Austria) impinging on a type-I BBO crystal ( $\beta$ -BaB<sub>2</sub>O<sub>4</sub>, Castech, China, cut angle 34°, 4-mm thick). The light from single twin coherence areas was delivered through two multimode optical fibers to two hybrid photodetectors (HPD, R10467U-40, Hamamatsu, Japan) and then amplified, synchronously integrated and digitized. Sequences of 50,000 subsequent laser shots at different values of the pump intensity were recorded. Raw data were analyzed by the self-consistent procedure explained in Refs. 9 and 10 so as to obtain the shot-by-shot determination of the number of detected photons, and hence the mean value  $\langle \hat{m} \rangle$ , the number of modes  $\mu$  and the quantum efficiency  $\eta$  directly from the experimental data.

The multimode thermal state was generated by passing the second harmonics output of the Nd:YLF laser through a rotating ground-glass plate and selecting by a pinhole a number of speckles in the far field (see Ref. 20). The number of modes can be modified by changing the size of the pin-hole.

Finally, the D-PHAV state was obtained superimposing a coherent portion of the second harmonics output of the Nd:YLF laser to another portion of the same beam whose phase was phase-averaged by moving a mirror mounted on a piezoelectric movement.<sup>16</sup> The characterization of this state in terms of photon statistics has been presented elsewhere.<sup>21</sup> In this paper we consider the case of a balanced state, where the contributions of the displacement and the phase-averaged state were equal.

To obtain a classical bipartite state,<sup>22</sup> either the multimode thermal state or the D-PHAV<sup>23</sup> were sent to a 50% beam splitter, whose output light was collected by two multimode optical fibers and sent to the same detection chain described above. In Fig. 1 we plot a sketch of the experimental setups.

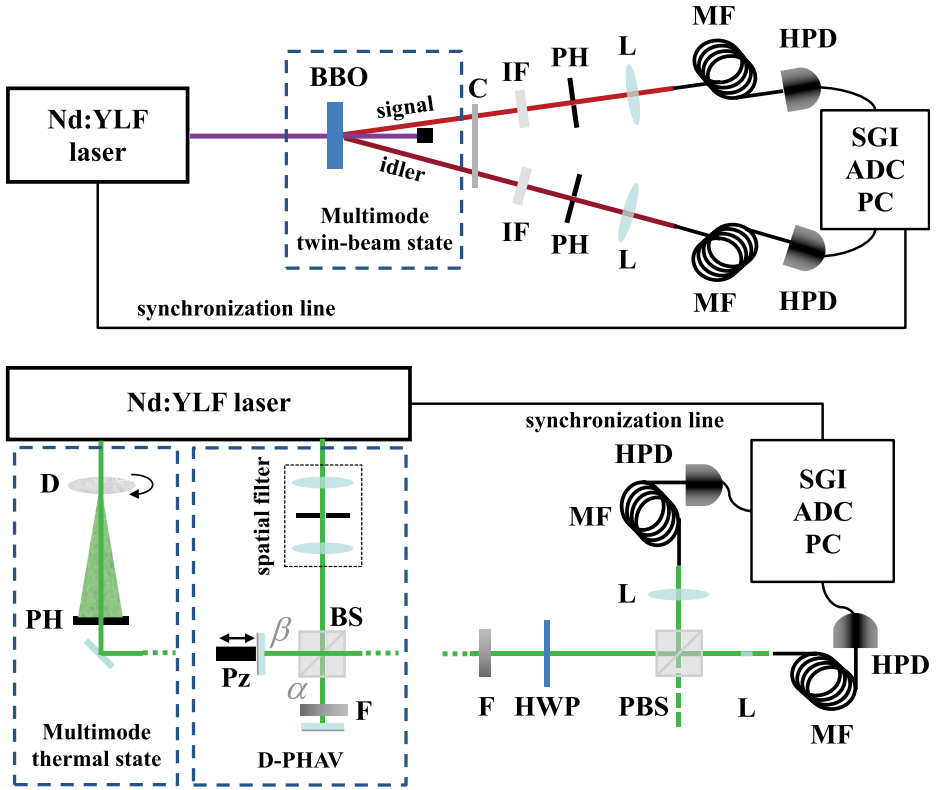


Fig. 1. Schematic diagram of the experimental setups to generate the states described in the text. Upper part: twin-beam state; lower part: multimode thermal state and D-PHAV. BBO: nonlinear crystal; C: cut-off filter; IF: interference filter; L: lens; PH: pin-hole; D: diffusing ground-glass plate; Pz: piezo-movement; BS: beam splitter; HWP: half-wave plate; PBS: polarizing beam splitter; MF, multimode optical fiber; HPD: hybrid photodetector plus amplifier; SGI: synchronous gated integrator; ADC+PC: digitizing PC board.

In Fig. 2 we plot the experimental data obtained by evaluating  $\Gamma_{\hat{m}}^{jk}$  up to the fourth order for a multimode TWB (black dots), a single mode thermal beam (gray dots) and a D-PHAV (dark-gray dots), as a function of the mean number of detected photons per mode. Superimposed to the experimental data we also plot the theoretical expectations (lines) calculated according to Eq. (5) by using Eqs. (3) or (4) in which the values of  $\langle \hat{m} \rangle$ ,  $\mu$  and  $\eta$  are directly obtained from the experimental data (see the figure caption for the details).<sup>11,12</sup> The agreement of experimental data with theory is very high.

From the results it is clear that the twin beam state is always more correlated than the classical states and that the amount of correlations increases with the order. Note that at the lowest order the multimode twin-beam state has almost the same amount of correlations as the single-mode thermal state, which is the most correlated classical state. At increasing correlation order, the difference between these two classes of

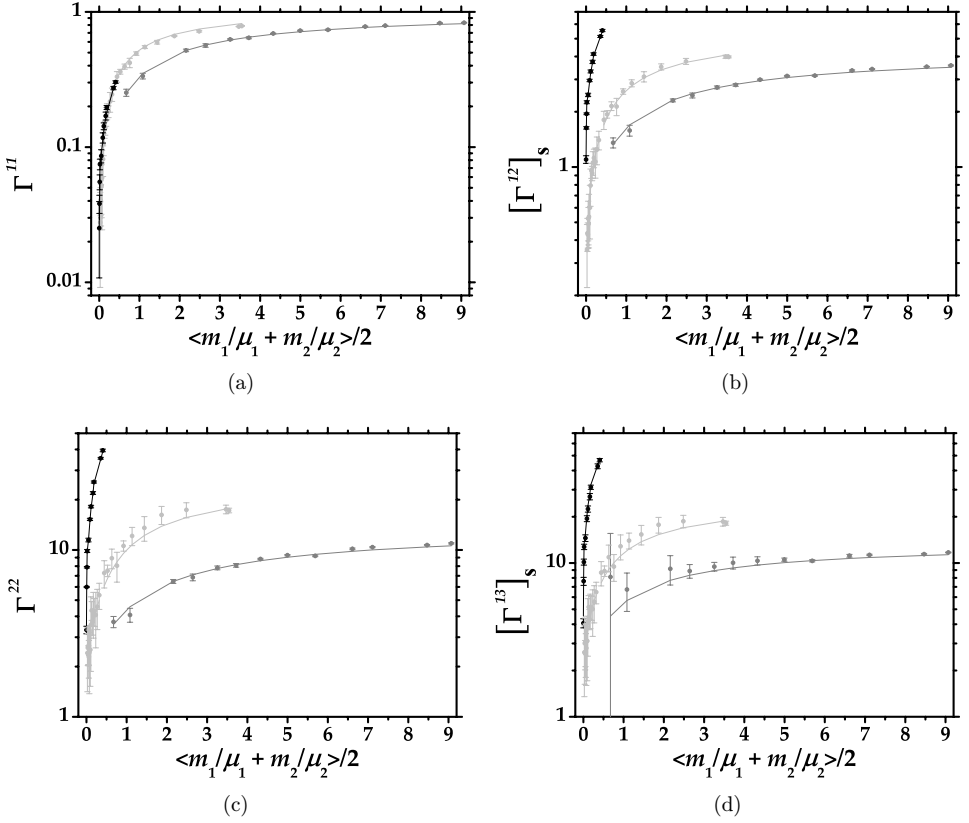


Fig. 2. High-order correlation functions plotted as functions of the mean number of detected-photons per mode. In each panel, black dots are the data for the multimode twin beam ( $\mu \sim 150$  on the average and  $\eta \sim 0.056$ ), light-gray dots are data for single-mode thermal state and dark-gray dots for single-mode D-PHAV; lines are the theoretical expectations. Panel (a):  $\Gamma_{\bar{m}}^{11}$ ; Panel (b):  $[\Gamma_{\bar{m}}^{12}]_s$ ; Panel (c):  $\Gamma_{\bar{m}}^{22}$ ; Panel (d):  $[\Gamma_{\bar{m}}^{13}]_s$ .

states becomes more and more evident. As expected, the D-PHAV is the less correlated at any order.

In Fig. 3 we plot the comparison between the two-mode thermal field (empty circles) and the D-PHAV (black dots) together with theoretical expectations (lines). In agreement with the analytical expressions in Eq. (5), the data for  $\Gamma^{11}$  coincide for the two states while become different for higher order correlations. This gives us a tool to discriminate among unknown states having the same mean value.

Finally, in Fig. 4 we apply the nonclassicality criterion introduced in Ref. 8 to the measured states: not surprisingly only the multimode twin-beam state results to be nonclassical. The fact that also a non-trivial classical state such as the D-PHAV respects the criterion of Ineq. (6) reinforces its validity.

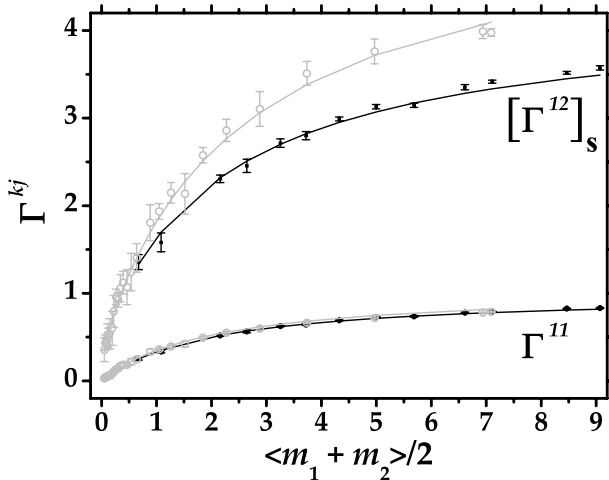


Fig. 3. High-order correlation functions  $\Gamma_m^{11}$  and  $[\Gamma_m^{12}]_s$  for D-PHAV (black dots) and two-mode thermal states (light-gray empty circles).

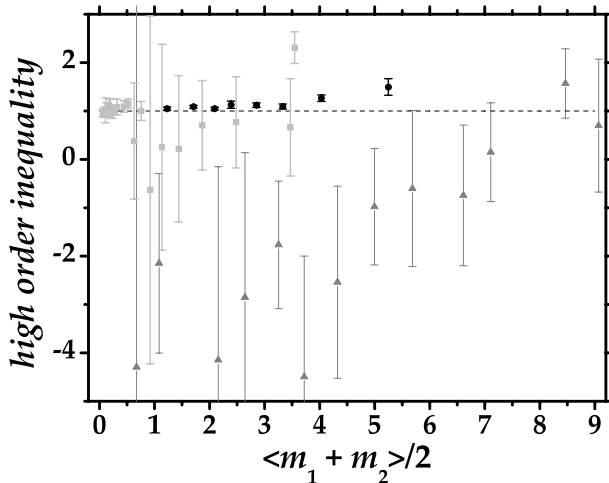


Fig. 4. Nonclassicality criterion of Ineq. (6) for a multimode twin-beam state (black symbols), single-mode thermal state (light-gray symbols) and D-PHAV (dark-gray symbols).

#### 4. Conclusions

In conclusion, we have defined new correlation functions derived on the basis of the detected-photon high order correlation functions that can be accessed by direct detection. We have calculated the analytical expressions of these functions for several classical and non-classical states, and in particular for the new class of D-PHAV, that is particularly interesting for applications to quantum-information protocols. We

have demonstrated that high-order correlations can indeed be very useful to discriminate among different states. The experimental results are in very good agreement with theory and suggest the possibility of using our experimental scheme for the characterization of quantum states for quantum technology.

## Acknowledgments

This work has been supported by MIUR (FIRB “LiCHIS” - RBFR10YQ3H).

## References

1. R. J. Glauber, *Phys. Rev.* **130** (1963) 2529.
2. L. Mandel and E. Wolf, *Optical Coherence and Quantum Optics* (Cambridge University Press, Cambridge, England, 1995).
3. W. Vogel, *Phys. Rev. Lett.* **100** (2008) 013605.
4. K. W. C. Chan, M. N. O’Sullivan and R. W. Boyd, *Optics Lett.* **34** (2009) 3343.
5. X.-H. Chen et al., *Optics Lett.* **35** (2010) 1166.
6. T. Iskhakov et al., *Eur. Phys. J. Special Topics* **199** (2011) 127.
7. M. Bondani, A. Allevi and A. Andreoni, *Eur. Phys. J. Special Topics* **203** (2012) 151.
8. A. Allevi, S. Olivares and M. Bondani, *Phys. Rev. A* **85** (2012) 063835.
9. M. Bondani, A. Allevi, A. Agliati and A. Andreoni, *J. Mod. Opt.* **56** (2009) 226.
10. A. Andreoni and M. Bondani, *Phys. Rev. A* **80** (2009) 013819.
11. A. Allevi et al., *Europhys. Lett.* **92** (2010) 20007.
12. A. Allevi, A. Andreoni, M. Bondani, M. G. Genoni and S. Olivares, *Phys. Rev. A* **82** (2010) 013816.
13. H.-K. Lo, X. Ma and K. Chen, *Phys. Rev. Lett.* **94** (2005) 230504.
14. M. Curty, T. Moroder, X. Ma and N. Lütkenhaus, *Optics Lett.* **34** (2009) 3238.
15. M. Curty, X. Ma, B. Qi and T. Moroder, *Phys. Rev. A* **81** (2010) 022310.
16. A. Allevi, S. Olivares and M. Bondani, Manipulating the non-Gaussianity of phase-randomized coherent states, *Opt. Express* **20** (2012) 24850.
17. R. J. Glauber, *Quantum Optics and Electronics* (Gordon & Breach, New York, 1965).
18. D. Klyshko, *Physical Foundation of Quantum Electronics* (World Scientific Publishing, Singapore, 2011).
19. G. Brida et al., *Phys. Rev. A* **83** (2011) 063807.
20. F. T. Arecchi, *Phys. Rev. Lett.* **15** (1965) 912.
21. M. Bondani, A. Allevi and A. Andreoni, *Adv. Sci. Lett.* **2** (2009) 463.
22. A. Allevi, M. Bondani and A. Andreoni, *Optics Lett.* **35** (2010) 1707.
23. A. Allevi, F. A. Beduini, M. Bondani and A. Andreoni, *Int. J. Quantum Inform.* **9** (2011) 103.